Available online at www.sciencedirect.com

SciVerse ScienceDirect

journal homepage: www.elsevier.com/locate/he

Multivariable 2-sliding mode control for a wind energy system based on a double fed induction generator

C.A. Evangelista, F. Valenciaga, P. Puleston*

CONICET and LEICI, Faculty of Engineering, National University of La Plata, C.C.91, (1900) La Plata, Argentina

ARTICLE INFO

Article history:
Received 9 September 2011
Accepted 12 December 2011
Available online 2 January 2012

Keywords:
Wind energy
Sliding modes
Multivariable systems
Power control

ABSTRACT

The purpose of this paper is to present a control strategy using Multiple Input/Multiple Output (MIMO) Second Order Sliding Modes (SOSM) for a grid-connected variable-speed Wind Energy Conversion System (WECS). The latter is based on a Double Fed Induction Generator (DFIG) in a bidirectional configuration with slip power recovery. Its points of operation can be electronically controlled and, with them, two independent control objectives can be stated. Thus, a control is designed to maximize the energy captured from the wind and to regulate the stator reactive power, contributing to the compensation of the power factor according to grid requirements.

The proposed technique can be applied to nonlinear MIMO systems and allows to make a separate design for each component of the controller. For these designs the Super-Twisting algorithm is employed in this work, which possesses excellent properties regarding simplicity of implementation and online operation, and robustness against uncertainties and external disturbances.

Finally, representative simulation results are presented and analyzed.

1. Introduction

The total wind installed capacity has been growing at a rate of 25% every year during the last decade, reaching 196GW worldwide by the end of 2010. Nowadays, wind power generate around 2.5% of the global electricity consumption [1].

The main reasons for this growth consist mainly in the general concern about climate change and environmental harming caused by traditional energy sources, as well as the wide availability of the wind and fossil depletion. Moreover, this industry has been supported by the global impulse it has received regarding investment, research and technological development of WECS. Such impulse is focused upon power yield optimization and reduction of loads and mechanical efforts, increasing thus the reliability and the life span of the whole system and reducing the cost of production of the generated energy. Among the topmost subjects under research are the improvements on the generator, drive train and power electronics, the search for new materials and designs for the wind turbines, the use of statistic signal processing techniques to estimate parameters or variables of interest, and the exploration and development of novel control strategies [2].

Related to the latter, the use of control techniques based on Sliding Modes (SM) is to be mentioned. Their several interesting characteristics make them attractive to deal with these kinds of systems, which rely on a random source as the wind, have nonlinear behavior and operate under external disturbances and uncertainties in the model parameters. Some of their main remarkable features are the following [3–7]:

- They can be applied to nonlinear as well as to linear systems.

* *Corresponding author*. Tel./fax: +54 2214259306.
E-mail address: cae@ing.unlp.edu.ar (C.A. Evangelista).

0360-3199/$ – see front matter Copyright © 2011, Hydrogen Energy Publications, LLC. Published by Elsevier Ltd. All rights reserved.
doi:10.1016/j.ijhydene.2011.12.080

- The designed controllers result extremely robust against several disturbances, uncertainties in the parameters and unmodeled dynamics.
- The control laws are relatively simple and easy to implement, entailing low real time computational burden.
- Some high order Sliding Mode algorithms have the additional advantage of synthesizing continuous control actions, consequently reducing mechanical efforts and chattering (high-frequency vibrations of the controlled system, main drawback of the first order SM originated in the practical impossibility of working at infinite switching frequency).

A SOSM based MIMO control is designed in this paper to maximize the extracted energy from the wind and to regulate the stator reactive power of a variable-speed grid-connected WECS based on a DFIG.

2. Brief description of the system and control objectives

Regarding wind generating systems connected to the grid, the ones based on DFIG which operate at variable speeds are among the most employed. One of them in a bidirectional topology with slip power recovery is considered in this work, and has been widely used in the last two decades.

This configuration consists of a wound rotor induction generator, where the windings of both stationary and rotating parts are connected to the grid, directly from the stator side and through a bidirectional converter on the rotor side, as it is schematically depicted in Fig. 1. Although it operates at variable speed, which can be higher or lower than the synchronous speed, it generates and transfers power at grid constant frequency. The mechanical power is fed in both through the stator and through the rotor, delivering thus more power than the rated and increasing the efficiency. The system can be electronically controlled by means of the frequency converter, allowing to choose the points of operation by modifying the amplitude and position of the spatial rotor voltage vector. Due to these two degrees of freedom, two independent control objectives can be stated and managed in this topology. Additionally, as the converter is fractional (i.e., it handles just the recovered power), it results smaller and of lower price than in other configurations.

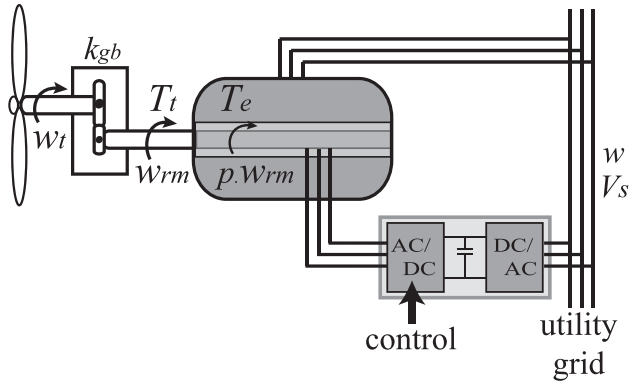

Fig. 1 – WECS-DFIG with slip power recovery.

In relation to the generation of power by the wind turbine, two zones can be distinguished within its range of operation, depending on the wind speed v, as shown in Fig. 2 [2,8].

While operating in the partial load zone, wind speeds between v_{cut-in} (lower speed at which the turbine starts generating) and v_{rated} (corresponding to the maximum power of the turbine), it is desirable to maximize the conversion efficiency, to obtain the maximum energy available in the wind. In a variable-speed WECS, the control in this zone is performed electronically, maintaining fixed the pitch angle of the blades. Between v_{rated} and $v_{cut-out}$ (upper limit speed from which the turbine should be disconnected to prevent damages) the extracted power should be limited to the rated value, which is usually regulated by a pitch controller.

The power a turbine captures is only a fraction of the power available in the wind. It can be written as [8]:

$$P_c = 1/2\pi\rho R^2 C_p(\lambda) v^3 \quad (1)$$

where ρ is the air density, R the blades length and $C_p(\lambda)$ the power coefficient of the WECS. This is a nonlinear function of the tip-speed ratio $\lambda \triangleq w_t R/v = w_{rm} R/(k_{gb} v)$, with w_t and w_{rm} the angular rotation speed of the turbine and of the generator shaft respectively, and k_{gb} the transmission ratio of the gear box. The C_p depends on the shape and geometrical dimensions of the rotor and the blades and, considering fixed pitch, presents a unique maximum for $\lambda = \lambda_{opt}$. The curve C_p–λ considered for the turbine in this work, modeled as $C_p(\lambda) = c_1(c_2/\lambda - 1)\exp(-c_3/\lambda)$ with c_1, c_2 and c_3 constants, is shown in Fig. 3, where its maximum has also been indicated.

The proposal in this paper consists in the application of a SOSM MIMO technique [9] to control the WECS with two objectives:

- maximize the extracted power, by tracking a torque reference to control the points of operation so that $\lambda = \lambda_{opt}$ for all wind speeds within the partial load zone, and
- tracking a reactive power reference in stator, contributing to compensate the grid power factor.

3. WECS model

A quite complete description of the WECS dynamics is attained by the five nonlinear differential equations usually referred as the Park model. Four of the equations consider the electric dynamics of both stator and rotor in a synchronously rotating direct-quadrature (d-q) frame and the fifth one accounts for the mechanical dynamics.

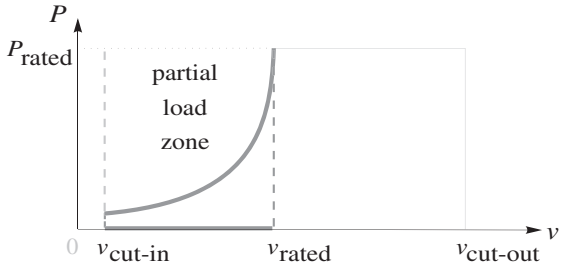

Fig. 2 – Zones of operation of a wind turbine.

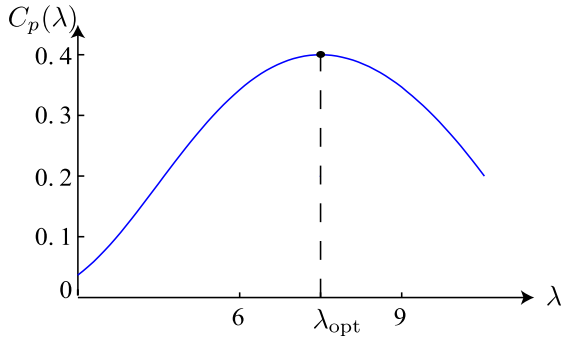

Fig. 3 – Power coefficient $C_p(\lambda)$.

Making some geometrical considerations and an electrical simplification (i.e., neglecting the stator resistance), a reduced order model can be obtained, which consists of three states accounting for the mechanical rotation speed and the electric rotor variables, whereas the stator currents are linked to them algebraically [10]:

$$\begin{cases} \dot{i}_{qr} = -\left(\dfrac{L_m V_s}{L_{eq}} + w i_{dr}\right)\left(1 - \dfrac{p}{w} w_{rm}\right) - \dfrac{R_r L_s}{L_{eq}} i_{qr} + \dfrac{L_s}{L_{eq}} v_{qr} \\ \dot{i}_{dr} = -w i_{qr}\left(1 - \dfrac{p}{w} + w_{rm}\right) - \dfrac{R_r L_s}{L_{eq}} i_{dr} + \dfrac{L_s}{L_{eq}} v_{dr} \\ \dot{w}_{rm} = \dfrac{1}{J}\left(T_t(v, w_{rm}) - \dfrac{3pL_m V_s}{2wL_s} i_{qr}\right) \end{cases} \quad (2)$$

$$i_{qs} = -\frac{L_m}{L_s} i_{qr} \quad (3)$$

$$i_{ds} = \frac{V_s}{wL_s} - \frac{L_m}{L_s} i_{dr} \quad (4)$$

where v_{qr} and v_{dr} are the voltage control inputs, p is the number of pole pairs of the generator, w and V_s are the line frequency and voltage, R_r is the rotor resistance, $L_{eq} = L_s L_r - L_m^2$, L_s and L_r are the leakage inductances of the stator and rotor windings respectively and J is the inertia of the whole combined rotating parts. T_e and T_t are the electrical resistant torque of the generator and the mechanical torque of the turbine, the latter rendered to the generator side through the gear box relation. Their expressions are:

$$T_e(i_{qr}) = \frac{3pL_m V_s}{2wL_s} i_{qr} \quad (5)$$

$$T_t(v, w_{rm}) = \frac{1}{k_{gb}} 0.5\pi\rho R^3 C_t\left(\frac{w_{rm} R}{k_{gb} v}\right) v^2 \quad (6)$$

where $C_t(\lambda) = C_p(\lambda)/\lambda$ is the torque coefficient of the turbine.

As for the stator reactive power, its expression in the three-equation model is:

$$Q = \frac{3pV_s^2}{2wL_s} - \frac{3pL_m V_s}{2L_s} i_{dr} \quad (7)$$

4. SOSM MIMO control

Second Order Sliding Modes aim to take to and maintain in zero a function of the system states and time, σ, and its first time derivative. This function is chosen according to the control objectives, so that they are accomplished when the condition $\sigma = 0$ is hold.

The points where $\sigma = \dot{\sigma} = 0$ in the state space determine the sliding manifold. The SOSM algorithms allow to synthesize a control law that takes the state trajectories onto the sliding manifold in finite time and robustly keeps the system operating in that condition. The algorithm which is employed in this work has the additional advantage of providing a continuous control action. In the sequel, the SOSM procedure is described, to design the control for a MIMO dynamic system of the form:

$$\dot{x} = \mathbf{F}(t, x) + \mathbf{G}(t, x)u \quad (8)$$

where $x \in \mathscr{R}^n$, $u \in \mathscr{R}^m$ are the control inputs, $f_i(\,)$ and $g_{ij}(\,)$ are $\mathscr{C}^1$-functions, for $i = 1, \ldots, n$; $j = 1, \ldots, m$.

The control objectives for system (8) are posed in m sliding variables, σ_i, $i = 1, 2, \ldots, m$, setting thus $\sigma(t, x) \in \mathscr{R}^m$. Each σ_i has to be a $\mathscr{C}^2$-function with relative degree well defined, i.e., matrix $\mathbf{B} = \sigma'_x \mathbf{G}$ must be nonsingular, where σ'_x denotes the partial derivative of σ with respect to x.

Given that the design procedure [9] requires matrix $\mathbf{B}$ to be upper triangular, the well-known Gauss procedure of variable exclusion is to be performed on $\mathbf{B}$, obtaining $\tilde{\mathbf{B}}$. It is necessary that $\tilde{\mathbf{B}}$ is bounded and nonsingular and all its elements maintain their sign unchanged for all t, x (this is, they are never zero), and the equivalent control $u_{eq}(t, x) \triangleq -(\sigma'_x \mathbf{G})^{-1}(\sigma'_t + \sigma'_x \mathbf{F})$ and its time derivative are also bounded. Then, it can be shown that each control component u_i can be associated to the corresponding component of the sliding variable σ_i and designed independently. This means that the MIMO SOSM design of the m-component control is simplified to design m SISO SOSM (Single Input/Single Output) controllers, using for each of them any of the already known SISO SOSM algorithms, like Twisting, Super-Twisting, "with a prescribed law of variation", Sub-Optimal, etc. [4,11,12,9].

5. SISO super-twisting control

As it was mentioned in the previous section, the MIMO SOSM design problem turns into m SOSM SISO designs. The interesting characteristics of the Super-Twisting algorithm [12] made it the selected option for the SISO controllers.

The Super-Twisting algorithm was developed to have a continuous and robust controller with the advantages of first order SM, but reducing its main drawback in sliding variables with a relative degree of 1, the chattering effect. It is very simple to implement and it has the advantage over other SOSM algorithms of needing to measure only the sliding variable and not requiring information of its time derivative, $\dot{\sigma}$.

Once chosen the functions $\sigma_i(t, x)$, their time derivatives can be written using (8) as:

$$\dot{\sigma}_i(t, x, u) = \underbrace{\left(\sigma'_{it} + \sigma'_{ix} f_i\right)}_{a_i(t,x)} + \underbrace{\left(\sigma'_{ix} g_{ii}\right)}_{b_i(t,x)} u_i \quad (9)$$

After this, positive constants U_{Mi}, C_i, Γ_{mi}, Γ_{Mi} and $q_i \in (0, 1)$ must be found such that:

$$\begin{cases} |\dot{a}_i(t,x)| + |\dot{b}_i(t,x)|U_{Mi} \le C_i \\ 0 < \Gamma_{Mi} \le |b_i(t,x)| \le \Gamma_{Mi} \\ \left|\dfrac{a_i(t,x)}{b_i(t,x)}\right| < q_i U_{Mi} \end{cases} \tag{10}$$

Under these conditions, the state trajectories will converge to the sliding manifold $\sigma = \dot{\sigma} = 0$ in finite time and the system will operate in SOSM on it if the following control action is applied, given by the Super-Twisting algorithm:

$$u_i = \zeta_i(-\lambda_i|\sigma_i|^{1/2}\text{sign}(\sigma_i) + u_{1i}) \tag{11}$$

$$\dot{u}_{1i} = \begin{cases} -u_i, & |u_i| > U_{Mi} \\ -\alpha_i \text{sign}(\sigma_i), & |u_i| \le U_{Mi} \end{cases} \tag{12}$$

where $\zeta_i = \text{sign}(b_i(t,x))$, called the influence sign, is fixed for every t, x, and the parameters α_i and λ_i verify:

$$\lambda_i > \sqrt{\frac{2}{\Gamma_{mi}\alpha_i - C_i}} \frac{\Gamma_{mi}\alpha_i > C_i}{\dfrac{(\Gamma_{mi}\alpha_i - C_i)\Gamma_{Mi}(1+q_i)}{\Gamma_{mi}^2(1-q_i)}} \tag{13}$$

The inclusion of bounded perturbations in the equations and their consideration in the computation of the bounding constants in (10) guarantees the robustness of the designed controllers against the accounted disturbances.

6. Design of MIMO Controller for the WECS

When the system is operating at the points where $\lambda = \lambda_{opt}$, that is, where the extracted power is maximum, the mechanical torque of the turbine equals

$$T_{t_{opt}}(w_{rm}) = \frac{\pi\rho R^5 C_{p_{max}}}{2k_{gb}^3\lambda_{opt}} = k_o w_{rm}^2 \tag{14}$$

If the electrical torque is compelled to track this $T_{t_{opt}}$, which varies with the wind speed, the system is forced to operate on the points of maximum captured power points, where $w_{rm} = \lambda_{opt}k_{gb}\nu$.

Considering the mentioned condition and Eq. (5) for the first control objective and using (7) for the second, the sliding variables are selected as:

$$\sigma_1 = T_{t_{opt}} - T_e = k_o w_{rm}^2 - \frac{3pL_m V_s}{2wL_s} i_{qr} \tag{15}$$

$$\sigma_2 = Q_{ref} - Q = Q_{ref} - \frac{3pV_s}{2L_s}\left(\frac{V_s}{w} - L_m i_{dr}\right) \tag{16}$$

The total time derivatives of (15) and (16) can be written using (2) as functions of the states:

$$\begin{aligned} \dot{\sigma}_1 &= 2k_o w_{rm}\dot{w}_{rm} - \frac{3pL_m V_s}{2wL_s}\dot{i}_{qr} \\ &= a_1(t, i_{qr}, i_{dr}, w_{rm}) + b_1(t, i_{qr}, i_{dr}, w_{rm})v_{qr} \end{aligned} \tag{17}$$

$$\dot{\sigma}_2 = \dot{Q}_{ref} + \frac{3pV_s L_m}{2wL_s}\dot{i}_{dr} = a_2(t, i_{qr}, i_{dr}, w_{rm}) + b_2(t, i_{qr}, i_{dr}, w_{rm})v_{dr} \tag{18}$$

with

$$\begin{aligned} a_1 = {} & \frac{3pL_m V_s}{2wL_s}\left(\frac{L_m V_s}{L_{eq}} + \frac{R_r L_s}{L_{eq}} i_{qr} + (w - pw_{rm}) - \frac{pL_m V_s}{wL_{eq}} w_{rm}\right) \\ & + \frac{2k_o w_{rm}}{J}(T_t - T_e) \end{aligned} \tag{21}$$

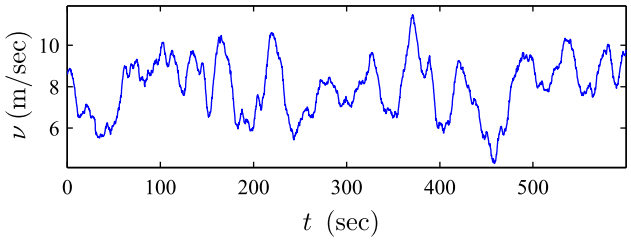

Fig. 4 – Wind speed time profile.

$$b_1 = -\frac{3pV_s L_m}{2wL_{eq}} \tag{22}$$

$$a_2 = \dot{Q}_{ref} + \frac{3pL_m V_s}{2L_s}\left((w - pw_{rm}) - \frac{R_r L_s}{L_{eq}} i_{dr}\right) \tag{23}$$

$$b_2 = \frac{3pV_s L_m}{2L_{eq}} \tag{24}$$

As it can be observed, in the case of the WECS described by the third order model given by (2) and for the selected sliding manifold, the time derivatives of the sliding variables depend each on one of the control inputs, v_{qr} and v_{dr}. Consequently, the matrix **B** mentioned in Section 4 is in this case a diagonal matrix, a particular case of an upper triangular one, not being necessary to perform the Gauss procedure.

Then, the bounding constants stated in (10) and the influence signs appearing in (11), necessary to design v_{qr} and v_{dr}, are to be found directly for (21)–(24). To get the bounds, a thorough analysis of the derived equations was carried out, complemented with computer simulations of the system operating within the partial load zone, fed with varied wind profiles and several reactive power references. In both cases, the analytical evaluation and the simulations, it was taken into consideration the effect of external disturbances as well as errors in the parameters of the models, such as variations in the electric resistances and in the electromagnetic inductances up to 10% of their rated values, and in the grid voltage and frequency up to 10% and 2% of their rated values, respectively. Finally, it was determined:

$$\begin{aligned} U_{M1} = {} & 300;\ q_1 = 0.7;\ C_1 = 51,100;\ \zeta_1 = -1;\ \Gamma_{m1} = 1600; \\ & \Gamma_{M1} = 2000;\ U_{M2} = 300;\ q_2 = 0.1167; \\ & C_2 = 2,876,000;\ \zeta_2 = +1;\ \Gamma_{m2} = 694,000; \\ & \Gamma_{M2} = 7 \times 10^5 \end{aligned} \tag{25}$$

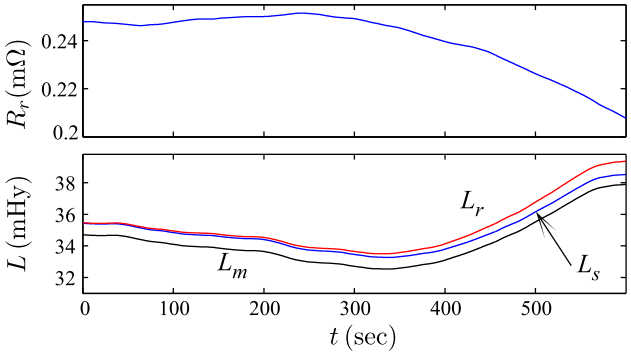

Fig. 5 – Time variation of electromagnetic parameters.

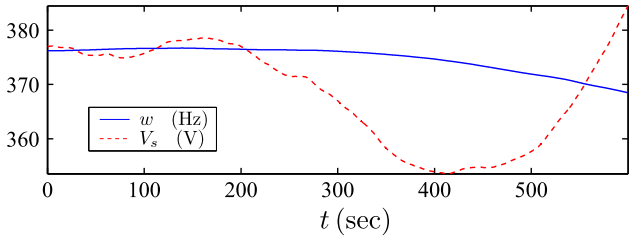

Fig. 6 – Time variation of grid parameters.

7. Simulations and results

The final tuning of the parameters for each component of the MIMO controller was set after new simulations. Maintaining the system in the partial load zone and under the same kind of disturbances, the fine tune was made prioritizing the reduction of mechanical efforts and chattering. The resulting selection was:

$$\alpha_1 = 60;\ \ \lambda_1 = 4.5;\ \ U_{M1} = 300 \tag{26}$$

$$\alpha_1 = 10;\ \ \lambda_1 = 0.1;\ \ U_{M2} = 300 \tag{27}$$

It is important to point out that although the computation of the bounding constants and the selection of the values of the parameters are not simple processes, they are made off-line during the tuning procedure. The online operation of the controllers, on the contrary, is quite simple.

Some results obtained in a representative simulation are shown and discussed in this section. They correspond to the WECS operating for 10 min under realistic conditions within the partial load zone, controlled according to the proposed strategy, with the controller developed in the previous sections. The wind speed profile that was used is presented in Fig. 4.

Fig. 5 shows the time variations of the electromagnetic parameters appearing in the third order model. The value of the rotor resistance is displayed in the upper box, while the values of the leakage inductances and of the magnetic coupling are in the box at the bottom.

The variations of the grid parameters are presented in Fig. 6. The variations of the parameters in the simulations lie within the range considered for each one in the design stage.

The electrical resistant torque of the generator, T_e and the torque reference being tracked, $T_{t_{opt}} = k_o w_{rm}^2$, are depicted in Fig. 7. The overlapping of both curves indicates the accomplishment of the first sliding objective, given by (15). The error in $\sigma_1 = T_{t_{opt}} - T_e$ is kept below 1×10^{-3} N m despite the disturbances, proving the robustness of the control algorithm.

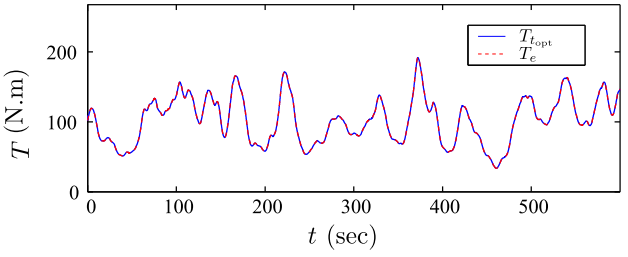

Fig. 7 – Electrical torque and torque reference.

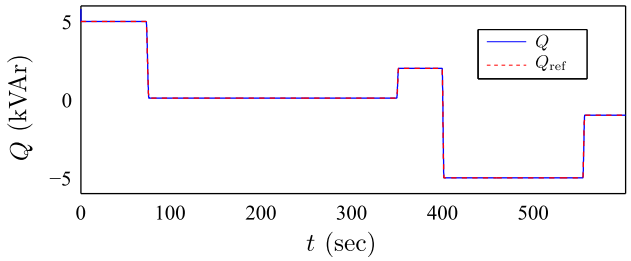

Fig. 8 – Reactive stator power and its reference.

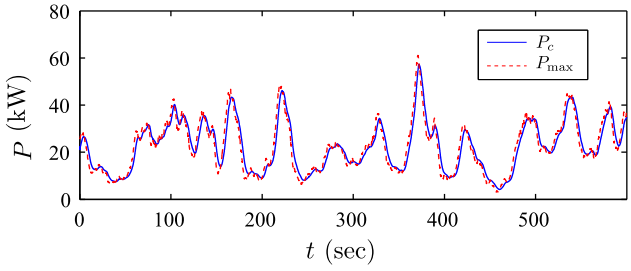

Fig. 9 – Captured and maximum available power.

Finally, the power profiles of the controlled machine can be seen in Figs. 8 and 9. Fig. 8 presents the temporal variations of the stator reactive power, Q, and of the reactive power reference, Q_{ref}. One curve is exactly over the other, showing the successful achievement of the second sliding objective, $\sigma_2 = 0$ ($\sigma_2 = Q_{ref} - Q$, in Eq. (16)). The accuracy and robustness of the controller is shown in the small error attained while tracking the reference under the described perturbations, maintained below 0.1 VAr once operating in SOSM.

The captured power and the maximum power available in the wind are portrayed in Fig. 9. Instead of overlapping, which would indicate maximum extracted power, it can be observed the first curve is a kind of delayed version of the second. The reason for this resides mainly in the choice of the corresponding sliding variable based on torques, resulting in a lowpass tracking of the maximum power.

8. Conclusions

A controller for the active and reactive power of a grid-connected variable-speed WECS based on a DFIG has been designed in this work. The WECS was modeled considering the electric currents in the rotor and the mechanical rotation speed of the shaft. For the wind turbine operating at wind speeds in the range between v_{cut-in} and v_{rated}, a SOSM MIMO technique was utilised to design the two-component controller.

Each of these components was designed separately, based on a SOSM SISO algorithm, the Super-Twisting. One of them was designed to track a torque reference so that $\lambda = \lambda_{opt}$,

aiming to maximize the conversion efficiency. The other, to track a reactive power reference in stator, contributing to the compensation of the grid power factor.

To determine the bounding design constants, the system was thoroughly analyzed and simulated during the off-line tuning procedure, considering realistic operating conditions and several bounded disturbances. The reduction of mechanical efforts and chattering were prioritized when fine-tuning the controller. It should be pointed out that while the determination of the bounds is carried out off-line, the control law is rather simple and it can be easily implemented, therefore it operates online with low computational burden.

Finally, simulations of the controlled system operating in the partial load zone, under realistic working conditions, showed the achievement of both control objectives and the robustness against external disturbances and variations of the parameters of the models with respect to their rated values.

Appendix A. Rated values and other parameters

$V_s = 460\sqrt{2/3}$ V; $w = 2\pi 60$ rad/s; $P_r = 50$ HP; $p = 2$; $R_s = 82$ mΩ; $R_r = 228$ mΩ; $L_s = 35.5$ mHy; $L_r = 35.5$ mHy; $L_m = 35.7$ mHy; $\rho = 1.224$ kg/m^3; $J = 3.662$ kg m^2; $R = 7.3$ m; $k_{gb} = 25$; $C_{p_{max}} = 0.4$; $\lambda_{opt} = 7.5$; $c_1 = 9.5946$; $c_2 = 12$; $c_3 = 20$

REFERENCES

[1] Tech. Rep.World wind energy report 2010. World Wind Energy Association; 2011

[2] Munteanu I, Bratcu A, Cutululis N, Ceanga E. Optimal control of wind energy systems. London: Springer-Verlag; 2007.

[3] Sabanovic A, Fridman LM, Spurgeon S, editors. Variable structure systems: from principles to implementation. UK: IET; 2004.

[4] Bartolini G, Ferrara A, Levant A, Usai E. Variable structure systems, sliding mode and nonlinear control. chap. 17, On second-order sliding-mode controllers. Springer; 1999. 329–350.

[5] Edwards C, Fossas Colet E, Fridman L, editors. Advances in variable structure and sliding mode control. Berlin: Springer; 2006.

[6] Boiko I, Fridman L, Pisano A, Usai E. Analysis of chattering in systems with second-order sliding modes. International Journal of Control 2007;52(11):2085–102.

[7] Levant A. Sliding order and sliding accuracy in sliding mode control. International Journal of Control 1993;58(6):1247–63.

[8] Burton T, Sharpe D, Jenkins N, Bossanyi E. Wind energy handbook. England: John Wiley and Sons; 2001.

[9] Levant A. Mimo 2-sliding control design. In: European control conference, ECC'03. Cambridge: United Kingdom; 2003.

[10] Valenciaga F, Evangelista C. 2-sliding active and reactive power control of a wind energy conversion system. IET Control Theory & Applications 2010;4(11):2479–90.

[11] Levant A. Principles of 2-sliding mode design. Automatica 2007;43(4):576–86.

[12] Fridman L, Levant A. Sliding mode control in engineering. chap. 3. In: Higher order sliding modes. Marcel Dekker, Inc.; 2002. p. 53–101.